

Climate sensitivity of glaciers in southern Norway: application of an energy-balance model to Nigardsbreen, Hellstugubreen and Alfotbreen

J. OERLEMANS

Institute for Marine and Atmospheric Research, Utrecht University, Utrecht, The Netherlands

ABSTRACT. Three glaciers in southern Norway, with very different mass-balance characteristics, are studied with an energy-balance model of the ice/snow surface. The model simulates the observed mass-balance profiles in a satisfactory way, and can thus be used with some confidence in a study of climate sensitivity. Calculated changes in equilibrium-line altitude for a 1 K temperature increase are 110, 108 and 135 m for Nigardsbreen, Hellstugubreen and Alfotbreen, respectively. The corresponding changes in mass balance, averaged over the entire glacier area, are -0.88 , -0.715 and -1.11 m year⁻¹ (water equivalent).

Runs with an ice-flow model for Nigardsbreen, to which calculated mass-balance profiles are imposed, predict that the front will advance by 3 km for a 1 K cooling, and will retreat by as much as 6.5 km for a 1 K warming. The response to a 10% increase in precipitation would be a 2 km advance of the snout, whereas a 4 km retreat is predicted for a 10% decrease. This large sensitivity (as compared to many other glaciers) is to a large extent due to the geometry of Nigardsbreen.

INTRODUCTION

The impressive programme of mass-balance monitoring carried out by the Norges Vassdrags- og Energiverk (NVE, Norwegian Water Resources and Energy Administration) on Norwegian glaciers provides an interesting data base for the study of climate-glacier relationships. Large differences in climatic regime are found over relatively small distances, notably in southern Norway, and consequently equilibrium-line altitudes vary by about 700 m over a distance of 200 km. A comprehensive documentation of glacier investigations in southern Norway is provided by the *Atlas over Breer i Sør-Norge* (Østrem and others, 1988) and a series of NVE reports. The atlas contains a bibliography, in which these reports are listed.

In this paper, the large west-east gradient in equilibrium-line altitude (denoted by E in the following) is used to test an energy-balance model designed to simulate glacier mass balance. An earlier version of this model was used to simulate the mass-balance profiles of Hintereisferner and Kesselwandferner (Austrian Alps), in connection with a sensitivity study on mass-balance gradients (Oerlemans and Hoogendoorn, 1989). It has also been applied to the Greenland ice sheet, in an attempt to calculate the surface mass balance from climatological data (Oerlemans, 1991). The principal of this model is to integrate the energy-balance equation for the ice/snow surface in time, including a daily cycle, with prescribed boundary conditions derived from climatological data (air temperature, precipitation, cloudiness, altitudinal change of temperature and precipitation). To be able to do

meaningful sensitivity studies, the albedo has to be internally generated. This forms a major problem in modelling studies of the present type, as a fully satisfactory parameterization of how the surface albedo varies in space and time is not available.

In the standard form of the model, the specific mass balance M (net annual gain of mass at the surface, per unit area and expressed here in m water equivalent) is generated on a "one-dimensional grid", chosen in such a way that grid points are equidistant in terms of surface elevation h . E can then be determined by interpolation. If a glacier has a discrete elevation-area distribution $S(h_i)$, the mean specific mass balance B_n is obtained from:

$$B_n = \frac{1}{S_T} \sum_i M(h_i)S(h_i). \quad (1)$$

Here, the sum is taken over the entire glacier, where the index i refers to the elevation interval centered around h_i . S_T is the total glacier area.

Three glaciers have been selected for the present study. One is *Alfotbreen* ($E \approx 1200$ m), located in western Norway close to the Atlantic coast, and subject to a very maritime climate with extremely high annual precipitation (≈ 5 m). Another one is *Nigardsbreen* ($E \approx 1550$ m), the well-known outlet glacier from Jostedalbreen, the largest ice cap in Europe. The character of this glacier is still basically maritime, but precipitation is less and the annual temperature range somewhat larger. The third one is *Hellstugubreen* ($E \approx 1900$ m), situated in a more continental climatic setting.

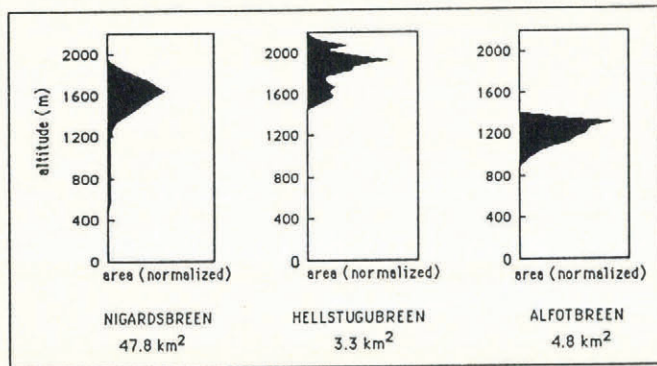


Fig. 1. Normalized hypsometries for the glaciers studied. Numbers at bottom give the total area.

The normalized hypsometry of the glaciers, taken from Haakensen (1982), is shown in Figure 1. By far the largest glacier is Nigardsbreen, with a narrow tongue (width ≈ 500 m) pushing far into a valley. Consequently, the melting rates on the tongue are very large ($\approx 10 \text{ m year}^{-1}$). Concerning mass turnover and hypsometry, Hellstugubreen has characteristics more similar to valley glaciers in the interior of the Alps (e.g. Hintereisferner). Alftobreen, on the other hand, is not a real valley glacier, but has a regular hypsometry (= area-elevation distribution). A tremendous amount of snow accumulates on this glacier, not only directly from precipitation, but also from snowdrift and avalanching. In many years, the winter mass balance on this glacier hardly depends on altitude, or even increases when going downward.

The most useful weather stations with sufficiently long records in this region are Bergen ($60^{\circ}12' \text{ N}$, $5^{\circ}19' \text{ E}$, 45 m), Fannaråken ($61^{\circ}31' \text{ N}$, $7^{\circ}54' \text{ E}$, 2064 m) and Dombås ($62^{\circ}04' \text{ N}$, $9^{\circ}07' \text{ E}$, 643 m). A summary of climatological data from these stations has been given by Müller (1987).

After a brief description of the energy-balance model and a discussion on the input data, three questions will be considered:

To what extent is the model able to simulate the large differences in mass-balance characteristics between Alftobreen, Nigardsbreen and Hellstugubreen?

Do sensitivity tests point to significant differences in the possible response of these glaciers to climate change?

How large should changes in the climate over the last few centuries have been to explain the pronounced variations in the front position of Nigardsbreen?

The last point will be studied by coupling the energy-balance model with an ice-flow model for Nigardsbreen, which was developed earlier (Oerlemans, 1986).

THE ENERGY-BALANCE MODEL

As a number of modifications have been made to the energy-balance model described in Oerlemans and Hoogendoorn (1989), a brief but full description of the

version used here is given below. The energy-balance equation at the surface forms the basis for the calculation of the mass balance. The temperature profile in the upper layers of the glacier is not calculated but an arrangement is made to deal with refreezing in spring/early summer. The basic equations read:

$$\psi = (1 - \alpha)G + I_{in} + I_{out} + H_s + H_l \quad (2)$$

$$M = \int_{\text{year}} \left\{ (1 - f) \min(0; -\psi L) + P^* \right\} dt. \quad (3)$$

In Equation (2), the energy balance is denoted by ψ and consists of absorbed solar radiation (α is albedo, G global radiation), incoming and outgoing longwave fluxes (I_{in} and I_{out}), and the turbulent fluxes of sensible and latent heat (H_s and H_l). It is assumed that melting occurs at the surface as soon as the energy balance becomes positive. L is the latent heat of melting. In Equation (3), f is the fraction of the meltwater that refreezes and does not contribute to mass loss. The accumulation rate is denoted by P^* . In all experiments described further on a precipitation-rate constant through the year is used. P^* is then set to zero when air temperature is above 2°C , and equal to the annual mean precipitation rate otherwise. M denotes the annual specific mass balance, but in discussing results we will also use the cumulative mass balance at time t from day 300 (the starting date for the integration of Equation (3)). So, at day 300, the cumulative mass balance is always zero, and it becomes equal to the specific mass balance after 1 year of integration.

The calculation of the global radiation on an inclined surface of a valley glacier is very complicated. First of all, the effect of reflecting slopes is difficult to deal with. Secondly, diffuse radiation can make up a very large part of G , notably when mean cloudiness is large as it is in western Norway. Reflecting slopes and shading effects are ignored here. The partitioning among diffuse (G_{dif}) and direct (G_{dir}) depends linearly on cloudiness n . For total cloud cover 80% of the global radiation is diffuse, whereas for clear-sky conditions this is only 15%. The equations are:

$$G = \tau_a \tau_n (Q_{dif} + Q_{dir}) \quad (4)$$

$$Q_{dir} = [0.2 + 0.65(1 - n)] S \sin(\gamma + \gamma_s)$$

$$\text{if } \gamma + \gamma_s > 0 \text{ and } \gamma > 0$$

$$Q_{dir} = 0 \text{ otherwise}$$

$$Q_{dif} = [0.8 - 0.65(1 - n)] S \sin(\gamma) \text{ if } \gamma > 0$$

$$Q_{dif} = 0 \text{ if } \gamma \leq 0$$

$$S = 1353 \{ 1 + 0.034 \cos(2\pi N / 365) \} \text{ Wm}^{-2}.$$

Solar elevation is denoted by γ , the projection of the surface slope in the direction of the Sun by γ_s , S is the solar constant which varies through the year as the Earth-Sun distance changes (N is number of day from 1 January). The transmissivities τ_a (air molecules and aerosol) and τ_c (clouds) are approximated as:

$$\tau_a = (0.79 + 0.000024h) \left\{ 1 - 0.08 \frac{(\pi/2 - \gamma)}{\pi/2} \right\} \quad (5)$$

$$\tau_c = 1 - (0.41 - 0.000065h)n - 0.37n^2.$$

The approximation for clouds is chosen to fit the experimental results of Sauberer (1955; see also Greuell and Oerlemans (1986)), which were obtained in the Alps. The treatment of the albedo in the model will be discussed in a separate section.

The calculation of incoming longwave radiation follows an approach similar to Kimball and others (1982). Two contributions are distinguished: one from the clear-sky atmosphere (but originating from the lowest tens of meters of the atmosphere), and one (denoted by I_{cl}) originating at the base of clouds and transmitted in the 8–14 μm band (atmospheric window), i.e.

$$I_{in} = \epsilon_a \sigma T^4 + I_{cl}. \quad (6)$$

The atmospheric emissivity is written in terms of water-vapour pressure e_a (in Pa) and air temperature T (in K, 2 m above the surface):

$$\epsilon_a = 0.7 + 5.95 \times 10^{-7} e_a e^{(1500/T)} - 2.5 \times 10^{-5} h. \quad (7)$$

The decrease of atmospheric emissivity with altitude thus obtained (i.e. because vapour pressure and temperature normally decrease with altitude) appears to be somewhat less than generally observed (Müller, 1984). The last term in Equation (7) deals with this. The cloud contribution to the longwave-radiation balance is written as:

$$I_{cl} = n f \sigma T_{cl}^4. \quad (8)$$

Temperature of the cloud base is denoted by T_{cl} . The factor f is the product of cloud-base emissivity, mean fraction of radiation emitted in the atmospheric window, and transmissivity of air between surface and cloud base in the window. Although cloud height relative to the surface will not be constant, no attempt was made to take such effects into account. The information on cloudiness and cloud height is very limited anyway. In the light of this, a more detailed treatment is not justified. In all experiments described in this paper, f was set to a value of 0.25. I_{out} was simply taken as the radiation emitted by a black body at the melting point, i.e. 315.6 W m^{-2} . This value will overestimate the longwave balance if the skin temperature is below the freezing point. However, as the energy balance is only relevant when melting occurs, the assumption of zero surface temperature will only lead to a small error in the simulated mass balance (see also the discussion in Greuell and Oerlemans (1986)).

Turbulent fluxes over melting ice/snow surfaces can be quite large in spite of the stable atmospheric stratification normally encountered. Compared to other atmospheric boundary layers, much of the turbulent kinetic energy is concentrated in relatively small scales, and thus existing theory for stable boundary layers may underestimate the turbulent fluxes. As, over ice, for most cases surface roughness and climatological wind conditions are unknown, a constant exchange coefficient C is used in the hope that the bulk effect of the fluxes is captured. The equations read:

$$H_s = C(T - T_s) \quad (9)$$

$$H_l = 0.622 \frac{CL}{c_p} \frac{(e_a - e_{as})}{p}. \quad (10)$$

Here T_s is surface temperature, c_p is atmospheric

pressure and e_{as} is saturation vapour pressure over water (when $\psi > 0$) or ice (when $\psi < 0$). The approximations used are (in Pa; see e.g. Kraus, 1972):

$$e_{as} = 610.8 \exp \left\{ 19.85 \left(1 - \frac{273.16}{T} \right) \right\} \quad (\text{over water}) \quad (11)$$

$$e_{as} = 610.8 \exp \left\{ 22.47 \left(1 - \frac{273.16}{T} \right) \right\} \quad (\text{over ice}). \quad (12)$$

As the surface temperature is not calculated, T_s is replaced by the melting point. In Greuell and Oerlemans (1986), a comparison was made between a full calculation, in which temperature was actually resolved as a function of depth, and a calculation with surface temperature at the melting point all the time. The differences in accumulated melt appeared to be quite small.

In the calculations presented in this paper, a constant value for the exchange coefficient was used, namely $7 \text{ W m}^{-2} \text{ K}^{-1}$ (unless stated otherwise).

PARAMETERIZATION OF THE ALBEDO

Performance of an energy-balance model in simulating glacier mass balance depends to a large extent on the way albedo is treated. Albedo varies strongly in space and time, depending on the melt and accumulation history itself. There are significant feed-backs involved, implying that a mass-balance model designed to study the response to climate change must generate the albedo internally. This is difficult, however, as so many factors are involved. The albedo depends in a complicated way on crystal structure, ice and snow morphology, dust and soot concentrations, morainic material, liquid water in veins, water running across the surface, solar elevation, cloudiness, etc. The best one can do is to construct a simple scheme, in which the gross features broadly match available data from valley glaciers.

Accumulation of atmospheric dust and morainic material clearly is a very important factor. It is reasonable to assume that *the concentrations found at the surface depend on the location relative to the equilibrium line*, as this determines the annual mean vertical ice velocity at the surface. So, as a starting point we define a “background albedo profile”:

$$\alpha_b = 0.43 + \frac{0.18}{\pi} \arctg \left(\frac{h - E + 300}{200} \right). \quad (13)$$

Here h and E are in m. This can be seen as the albedo that would be approached when the melt season would last infinitely long. The constants appearing in Equation (13) have been found after much experimentation as giving good results (in terms of the simulation of the typical albedo pattern on a valley glacier at the end of the ablation season). The α_b profile is shown in Figure 2.

As snow on the lower parts of glaciers normally occurs in patches, it is realistic to make the increase of albedo a smooth function of snow depth d (in m water equivalent), in such a way that a smooth transition between α_b and the snow albedo is obtained. The expression used for α reads:

$$\alpha = \alpha_{sn} - (\alpha_{sn} - \alpha_b) e^{-5d}. \quad (14)$$

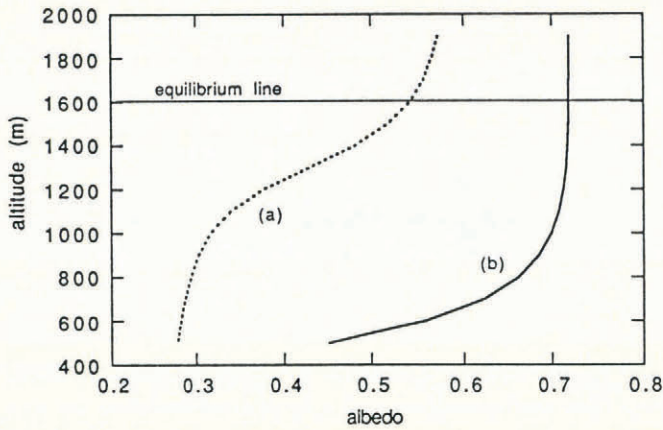


Fig. 2. Curve (a) shows the background albedo profile as formulated in Equation (10). The equilibrium-line altitude is set to 1600 m. The effect of an additional snow cover, increasingly linearly from 0.1 m at 500 m elevation to 1.5 m (water equivalent) at 1900 m elevation is illustrated by curve (b).

Here, snow albedo α_{sn} is assumed independent of the age of the snow, although age-dependence was in fact considered in the earlier study (Oerlemans and Hoogenboom, 1989). The justification for this assumption is that the modelling of precipitation is too schematic for a detailed treatment of age effects. To compensate for this simplification, the snow is assumed to have a standard age, and the value for α_{sn} is suitably reduced below that for fresh snow, namely 0.72.

REFREEZING

Meltwater that penetrates into the snowpack with a temperature below the melting point will refreeze and not run off. This process is dealt with by specifying that the fraction of melt energy involved in run-off, denoted by R , increases when the snow/ice temperature approaches the melting point. The equations used are:

$$R = \psi \exp(cT_{ice}) \tag{15}$$

$$H_{ice} = \psi - R = \psi(1 - \exp(cT_{ice})) \tag{16}$$

$$C \frac{dT_{ice}}{dt} = H_{ice} \quad (T_{ice} \leq 0). \tag{17}$$

Here H_{ice} is the heat flux into the upper ice/snow layer. This layer is assumed to have a heat capacity equivalent to 2 m of solid ice (with a density of 900 kg m^{-3}); its mean temperature is denoted by T_{ice} (in °C). The constant c determines how fast the fraction of melted snow that runs off approaches 1. Here c was set to 1 K^{-1} .

When the integration is started, normally at day 300, the ice temperature is set equal to the annual mean air temperature. This temperature can then only be changed by refreezing meltwater in the beginning of the ablation season. So, at higher elevations, where temperatures are lower, more snow has to be melted before the cold layer is heated up and significant run-off may start. The layer thickness of 2 m is rather ambiguous, but, concerning the amounts of energy involved, in line with the findings of Ambach (1963).

TECHNICAL ASPECTS AND INPUT DATA

The integration of the energy-balance model is performed with a 15 min time step to obtain a satisfactory resolution of the daily cycle. The starting date is day 300, i.e. at the end of October. This ensures that in most applications (northern mid- and high latitudes), the model simulation starts when the ablation season has more or less ended. Calculations are done simultaneously on a grid which is equidistant in altitude. The grid points may represent surfaces with different slope and exposure. The typical grid-point "distance" is 50 m of elevation for small glaciers and 100 m for large glaciers.

There are several reasons why the integration has to be extended over 2 or 3 years. First, the initial conditions cause transient effects which take over a year to die out. This applies in particular to the albedo ($\alpha = \alpha_b$ at $t = 0$). Secondly, the background albedo profile is tied to the height of the equilibrium line E , which can only be computed after a 1 year's integration; thus, at least a second year has to be simulated. In practice, it appears that the solution is in equilibrium after 3 years, and in most cases after 2 years (i.e. after one iteration). Care has to be taken concerning initial conditions: mass balance, accumulated melt, snow depth and ice temperature are initialized again every year, but albedo and equilibrium-line altitude not. This procedure is further illustrated in Figure 3.

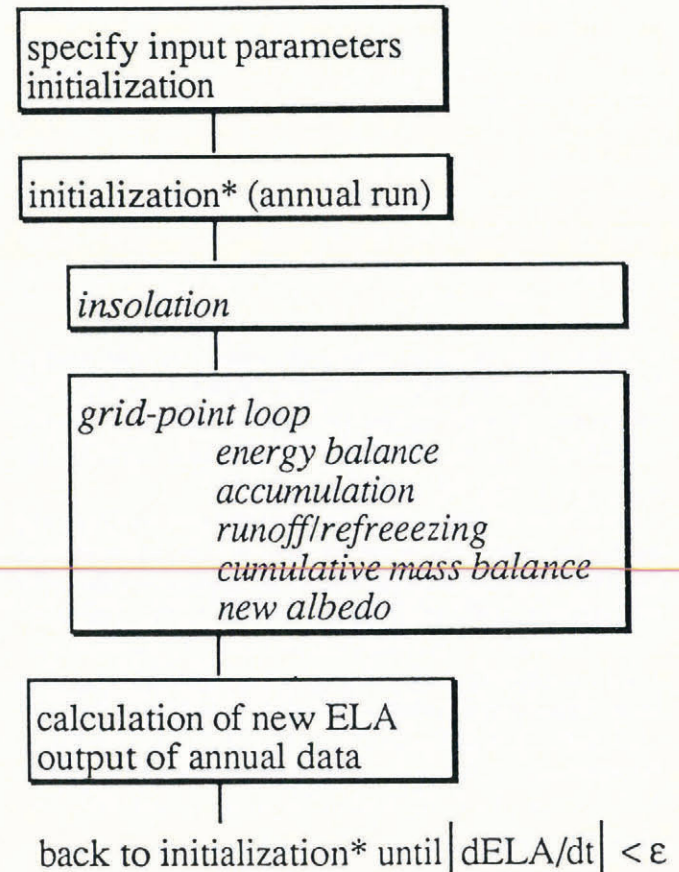


Fig. 3. Structure of the computer code. Two or three cycles of one simulated year are required to obtain a steady-state balance profile. After each year, some of the variables are initialized again (*, see text). Actual time integration over 1 year with 15 min time step is shown in italics.

Table 1. Input parameters for the mass-balance simulations

	Nigardsbreen	Hellstugubreen	Alfotbreen
Annual temperature range (°C)	16.0	16.0	14.0
Daily temperature range	6.0	6.0	6.0
Lapse rate (°C m ⁻¹)	0.0071	0.0071	0.0065
Cloudiness (fraction)	0.7	0.6	0.85
Cloud height (m)	2500	2500	2000
Relative humidity (%)	80	80	80
Annual precipitation (m)	2.3 + 0.0012 <i>h</i>	1.27 + 0.00066 <i>h</i>	7
Slope	0.05	0.1	0.2
Exposure (°)	160	0	40
Number of grid points	17	15	11
Grid-point distance	100	50	50

Meteorological input data needed to run the model are temperature and humidity at standard measuring height (= 2 m, also referred to as screen height), cloudiness and precipitation. As little information is available on humidity and cloudiness, these quantities are set equal to constant values for each glacier studied in the present paper (see Table 1). Air temperature is generated by assuming sinusoidal shapes for seasonal and daily variations:

$$T = M_T - \gamma_M h - A_T \cos[2\pi(N_{\text{day}} - 26)/365] - D_T \cos[2\pi(t - 3)/24]. \quad (18)$$

M_T is annual mean temperature reduced to sea level, and γ_M lapse rate of annual mean temperature. N_{day} is the day number (1 January corresponds to $N_{\text{day}} = 1$) and t local time in h. In all experiments discussed here the precipitation rate was kept constant through the year, but was allowed to depend on altitude.

Little material is available to determine the altitudinal gradients. However, there is one high-altitude climatological station in the region, which provides some information. This is Fannaråken at 2064 m above sea level.

A lapse rate calculated from a monthly climatology (taken from Müller, 1987) is shown in Figure 4. The

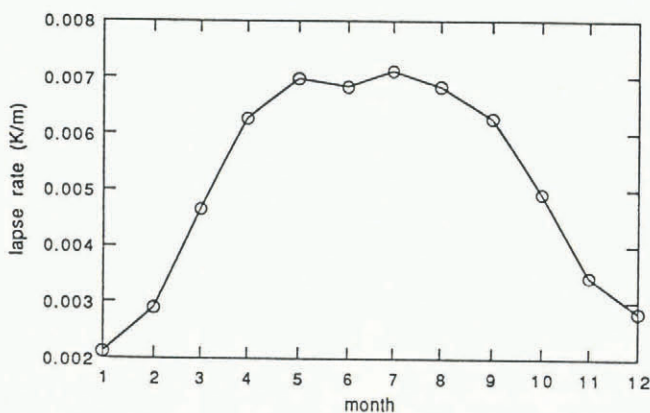


Fig. 4. Temperature lapse rate calculated from monthly temperatures at Dombås (643 m) and Fannaråken (2064 m).

extreme seasonal march is striking, but probably of little relevance to the present application of the energy-balance model. The small values of the lapse rate outside the summer season must be due to inversion conditions in the valley in which Dombås is located. Only in summer, when (moist) convective mixing is significant, does the lapse rate approach the value which is normally found in the mid-latitude atmosphere. Katabatic flows on glaciers are another feature that makes the use of the “Dombås–Fannaråken lapse rate” doubtful. Because of adiabatic warming, these flows tend to push the lapse rate to larger values all the time. Fortunately, some information is available on the summer lapse rate on Nigardsbreen, which will then also be used for Hellstugubreen. The values actually used are given in the discussion on the individual glaciers farther on.

The climatology from several stations (Müller, 1987), combined with the precipitation and run-off maps in Østrem and others (1988), reveals the following general features when going from west to east in the study area:

Annual precipitation on the higher ground decreases from over 4000 mm in the area of Alfotbreen to less than 2500 mm in Jotunheimen.

The altitudinal gradients increase (the valleys are more and more sheltered to the west).

Annual mean temperature, reduced to sea level, is fairly constant.

The annual temperature range increases significantly, from about 15 K at the Atlantic coast to 24 K in Jotunheimen.

At higher elevations, the annual temperature range is much smaller (Fannaråken: 15 K).

SIMULATION OF MASS-BALANCE PROFILES

To simulate the mass balance of Nigardsbreen, it seems best to take meteorological data obtained at Steinmannen

(research cabin at 1630m above sea level) as a basis. Mean summer temperature at this station is 3.8°C, and the lapse rate down to Jostedal appears to be 0.0071 K m⁻¹ (Østrem and others, 1976; Haakensen, 1982). This value is in notable agreement with the June–July–August values seen in Figure 4. As the summer lapse rate is the most important, this value was used throughout. The climatological precipitation is more difficult to obtain. The relation given in Table 1 is based on the map presented in Østrem and others (1988). In this table, the input data for the three glaciers are summarized. Some parameters have the same values for each glacier, as detailed information is not available.

Precipitation dominates the differences between the climatic regimes in which the glaciers are situated. The precipitation for Hellstugubreen is simply taken to be 55% of the precipitation for Nigardsbreen. This value was chosen because it yields a reasonable simulation and is in line with the precipitation map referred to above. On Alftobreen the winter mass balance is so large that this can only be explained by piling up of snow because of drift and avalanches. The model simulates both the winter mass balance and the annual mass balance well if the annual precipitation (thus including deposition of snow by other processes) is set to 7 m of water equivalent!

The simulated mass-balance profiles are shown in Figure 5, together with the observed mass balance

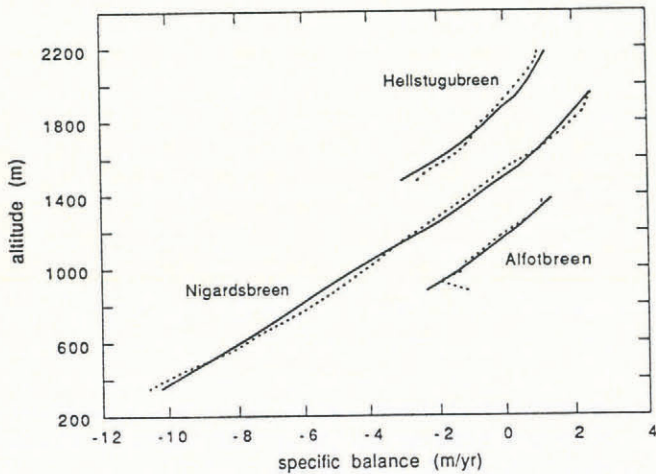


Fig. 5. Simulated mass-balance profiles (solid lines) compared to observations (dashed lines).

averaged over 24 years. Although some significant differences can be seen, the overall impression is that the model does a good job. A larger discrepancy between simulated and observed mass balance occurs for the lower reaches of Alftobreen. This is due to additional accumulation on the tongue, which is not taken into account in the model run shown. In the sensitivity experiments to be discussed later, an additional amount of mass of 2 m is put on the lowest grid point, and 1 m on the next grid point. This then gives a perfect match to the observations.

Figure 6 shows cumulative mass balance, from day 300 when the model balance year starts, and albedo as a function of altitude for some selected times, for the Nigardsbreen simulation. It can be seen that even after day 300 there still is some melting on the tongue. The mass-balance gradient on day 70 (the day with the largest value of the cumulative balance at the glacier tongue) is a direct reflection of the altitudinal gradient in the precipitation. On day 160 the cumulative mass balance at the uppermost grid point reaches its highest value (2.6 m). The smallest value at this grid point appears on day 250. So, according to the model, the firn area loses mass during about 100 d. It is obvious from these profiles that *it is very hard to use the concepts of winter and summer mass balances in discussing the model output*. This applies in particular to Nigardsbreen, where the altitudinal range is so large. The corresponding albedo profiles in Figure 6b look reasonable, but there are little data available to perform an objective test.

As considered explicitly by Kuhn (1979), the exchange coefficient for the turbulent fluxes has a strong influence on the mass-balance gradient. This is illustrated in Figure 7, where the results of two sensitivity experiments for Nigardsbreen are plotted: one with an exchange coefficient increased by 3 W m⁻² K⁻¹, and one with a uniform increase in precipitation of 20%. In both cases, the mass-balance gradient appears to increase. In fact, it is obvious that in this type of model simulation fine tuning can be done by adjusting precipitation and turbulent exchange within the ranges accepted (which are usually quite broad because of lack of detailed observations).

CLIMATE SENSITIVITY

There are many model constants and parameters that can

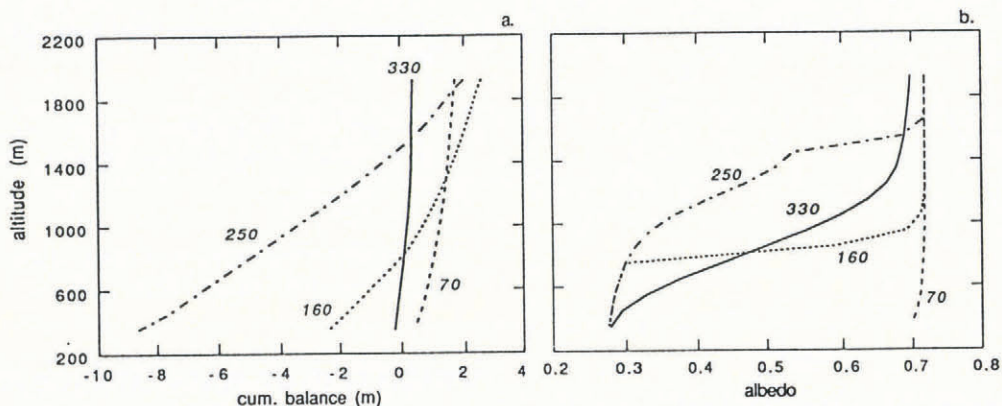


Fig. 6. Cumulative mass balance from day 300 at some selected days (a). The corresponding albedo profiles are shown in panel (b).

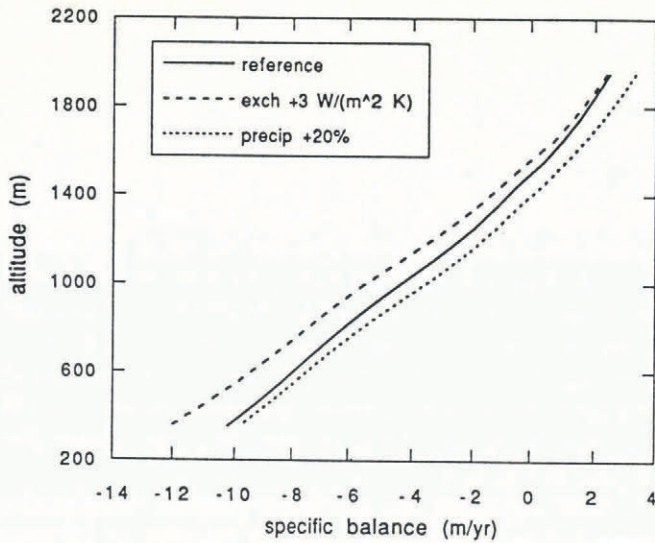


Fig. 7. A sensitivity experiment for the mass-balance profile of Nigardsbreen. In one case the turbulent exchange coefficient is increased by $3 \text{ W m}^{-2} \text{ K}^{-1}$; in the other case precipitation is 20% larger.

be varied but, as this was done extensively in Oerlemans and Hoogendoorn (1989), the analysis here will be restricted to annual mean air temperature and precipitation. In the discussion below, the word sensitivity is used to designate the change in mass balance or equilibrium-line altitude for a given change in climatic conditions. Figure 8 summarizes the results of a series of experiments, in which these quantities were systematically varied.

With regard to temperature, Alftobreen is by far the most sensitive glacier. Two factors are responsible for this: (1) the albedo feed-back is stronger when the winter snowpack is thicker and lasts longer, and (2) the absolute change in fraction of precipitation falling as snow is larger. It should be noted, however, that the treatment of rain in the model is extremely simple: it just runs off immediately! Hellstugubreen is the least sensitive glacier for opposite reasons, and Nigardsbreen is in between. It can be anticipated that other glaciers in the region have sensitivities lying in the range bounded by Alftobreen (extreme maritime) and Hellstugubreen (continental). So, most likely, differences in sensitivity are *within a factor of two*.

In terms of equilibrium-line altitudes, the results for

Table 2. Sensitivity of equilibrium-line altitude with respect to changes in annual mean temperature and precipitation

	dE/dM_T	dE/dP
	m K^{-1}	m \%^{-1}
Nigardsbreen	110	5.2
Hellstugubreen	108	6.7
Alftobreen	135	6.8
Mean value	118	6.2

the three glaciers differ less. In Table 2 values of dE/dM_T are listed. The mean value turns out to be 118 m K^{-1} , which is in line with many other studies. The fact that variability in E is much less than variability in B_n is not due to the hypsometries of the glaciers, but is the consequence of changing mass balance gradients.

Figure 8b shows how changes in precipitation affect the mean specific mass balance. Relative perturbations have been imposed, i.e. a percentage of the annual precipitation P for the particular glacier. So the absolute changes for the three glaciers are different. Also, in this approach smaller precipitation means a smaller absolute value of the altitudinal gradient. With regard to precipitation changes, Alftobreen shows the largest sensitivity again, although the differences between the glaciers are smaller now. The corresponding changes in equilibrium-line altitude are listed in Table 2. The mean value is 6.2 m \%^{-1} , implying that a 20% change in precipitation has roughly the same effect on the equilibrium-line altitude as a 1 K temperature change.

As noted earlier, mass-balance gradients change significantly when input parameters are varied. The largest sensitivity of the mass balance is found at lower elevations, which should *enhance the sensitivity of glacier-front position to climate change*. To investigate this point further, a few experiments were done with a numerical flow model for Nigardsbreen, developed earlier (Oerlemans, 1986). This model is of the vertically integrated type: it calculates mean ice velocity along a flow line, taking into account

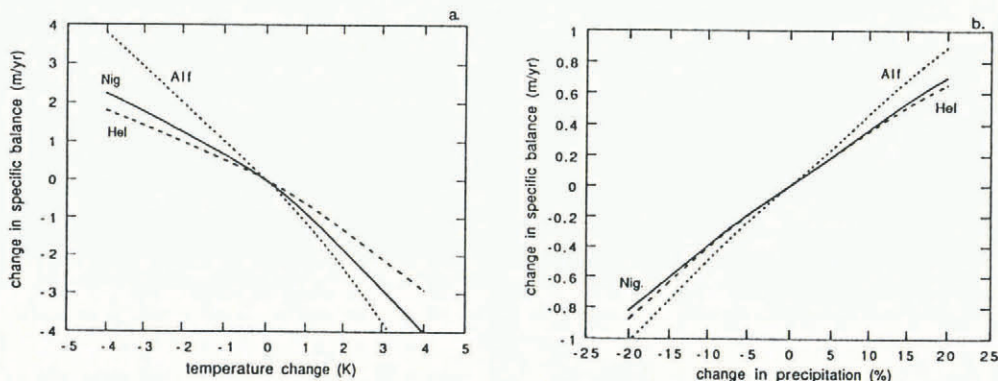


Fig. 8. Mean specific mass balance in dependence of a change in annual mean air temperature (a) and annual precipitation (b).

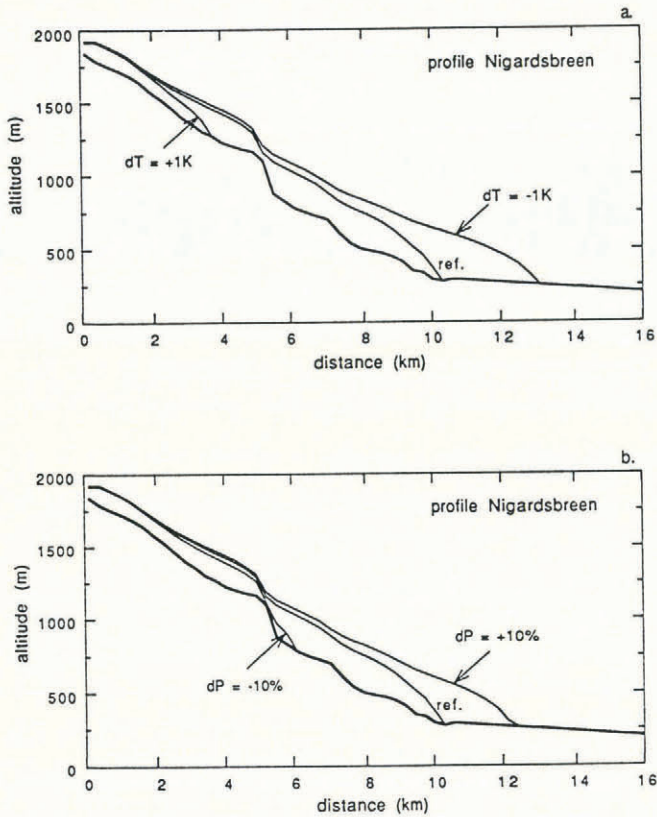


Fig. 9. Profiles of Nigardsbreen simulated with an ice-flow model. The curve labelled "ref" corresponds to the calculated mass-balance profile as shown in Figure 5. Equilibrium states are shown for perturbations in temperature (a) and precipitation (b), as indicated.

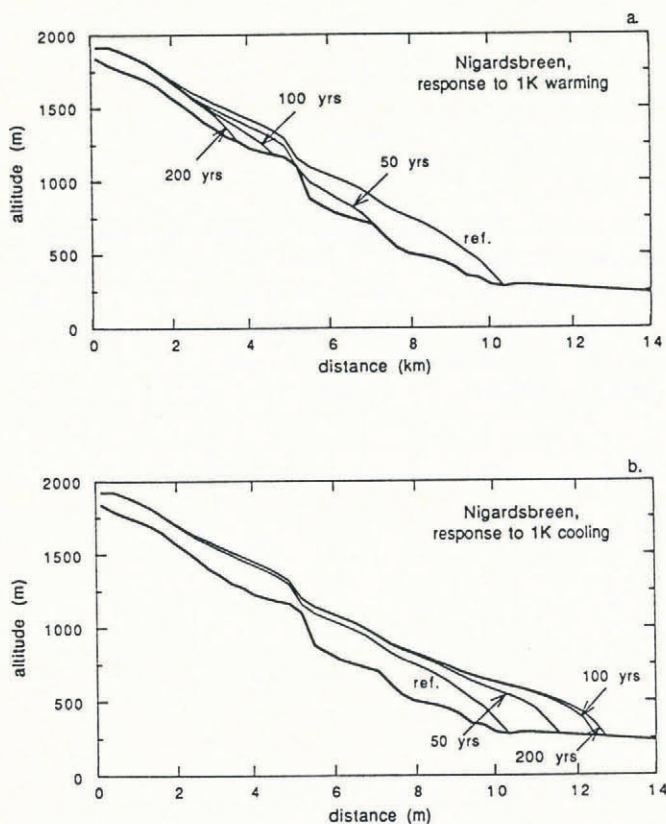


Fig. 10. Response of Nigardsbreen to a step change in annual mean temperature.

variations in the width of the glacier (depending on the width of the bed and ice thickness). The grid-point distance used is 300 m, giving sufficient resolution for the present purpose. For a further discussion on this model the reader is referred to the paper mentioned above.

The mass-balance model was coupled to the flow model in a simple way: a parabolic fit was made to the simulated mass-balance profiles (i.e. B_n as a function of surface elevation) and included in the flow model. So the feed-back of changing surface elevation on the mass balance was fully taken into account. In Figure 9, calculated equilibrium profiles are shown for some changes in climatic parameters. The reference case corresponds to the simulated mass-balance profile displayed in Figure 5.

The sensitivity of the front position to negative perturbations of the mass balance appears to be very large. A retreat of more than 6 km is predicted by the model for 1 K temperature increase. The advance for a 1 K cooling is less spectacular: about 3 km. Also, the ultimate retreat predicted for a 10% drop in precipitation is large: about 4 km. In this case, the tongue would take a stable position just below the icefall. In considering this large sensitivity, one should bear in mind, however, that the relative changes in total ice volume are much smaller as the bulk of the glacier surface is above 1500 m (see Fig. 1).

An idea on response times is provided in Figure 10. The 1 K warming or cooling has been imposed on the flow model as a step function, at the time that the glacier was in equilibrium with the reference mass balance. Calculated profiles are shown for 50, 100 and 200 years after introducing the climatic perturbation. In both cases, after 200 years of simulated time, the glacier front comes close to the corresponding equilibrium positions. After 50 years it is about half-way. In view of these results, it appears that the historic variations of the front position of Nigardsbreen, although quite large (≈ 4 km), can be explained by climatic changes that are relatively small.

The large sensitivity is mainly due to two factors. First, the hypsometry of Nigardsbreen plays an important role. The relatively narrow tongue, fed by a very large accumulation area, must respond strongly to small changes in the mean mass balance. In addition to this, the area of the ablation zone increases substantially when the equilibrium line goes up slightly. Secondly, the fact that the mass-balance gradient is larger/smaller for a warmer/cooler climate tends to enforce retreat/advance of the glacier snout.

This finding supports the view expressed in Oerlemans (1988), namely, that the amplitude of historic glacier variations can be better understood when higher temperature would imply larger mass-balance gradients.

CONCLUDING REMARKS

The energy-balance model used in this study appears to be capable of handling the large differences in mass-balance characteristics of glaciers found over a short distance in southern Norway. This gives credibility to the results of sensitivity experiments in which environmental parameters are varied.

Changes in the mean specific mass balance for

imposed temperature perturbations appear to be within a range that spans a factor of two. The model shows that maritime glaciers are most sensitive, both with respect to changes in temperature and precipitation. It is interesting to compare the present results with energy-balance calculations done earlier for other glaciers (for the Greenland ice sheet (Oerlemans, 1991); for Hintereisferner (Oerlemans and Hoogendoorn, 1989); and for three general classes of glaciers in the Alps (dry, intermediate, moist regime); Oerlemans, in press). The results are shown together in Figure 11. The upper panel shows changes in equilibrium-line altitude for a 1 K warming, the lower panel the corresponding changes in mean specific mass balance B_n . Values have been plotted as a function of the annual precipitation in the highest part of the accumulation area. Although the glacier hypsometry is different for all cases, a clear relation between annual precipitation and change in mean specific mass balance shows up. *This does not apply to the equilibrium-line altitude, however.* The lowest point in Figure 11b corresponds to the entire Greenland ice sheet. As in this case, roughly half of the ice loss is by calving, the comparison with the other calculations is a bit cumbersome. If one were to allow the Greenland ice sheet to have no calving, and thus a larger ablation zone, the sensitivity would increase.

A parabolic fit to the data points in Figure 11b gives:

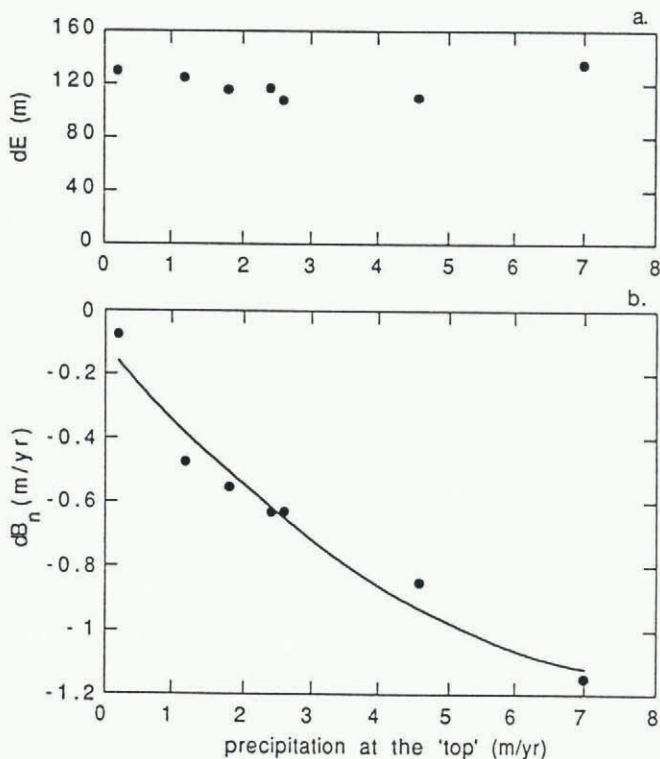


Fig. 11. A summary of results from energy-balance modelling of glacier mass balance. Calculations have revealed that precipitation in the accumulation area is the most important factor that determines the sensitivity of glacier mass balance for temperature changes. Shown here is the response to a 1 K warming in various climate regimes, ranging from the Greenland ice sheet (data point at left) to Alftobreen (data point at right). The upper panel gives the change in equilibrium-line altitude, the lower panel the change in mean specific mass balance (with a parabolic fit).

$$\delta B_n = -0.1087 - 0.2465P + 0.01457P^2 \text{ m year}^{-1}. \quad (19)$$

In principle, this relation combines two effects: (i) maritime glaciers are more sensitive than continental glaciers, and (ii) the hypsometry of maritime glaciers is different, i.e. the ablation zone extends further down into a warmer climatic environment. Some additional numerical experimentation with fictitious glacier geometries revealed that the first effect is far more important. It thus appears that Equation (19) can be used in estimating glacier wastage due to temperature change, for any climatic regime. For calving glaciers, however, additional corrections have to be made. A possibility would be to use the following expression instead of Equation (19):

$$\delta B_n = \frac{R_{\text{tot}}}{R_{\text{tot}} + C_{\text{tot}}} [-0.1087 - 0.2465P + 0.01457P^2] \text{ m year}^{-1}. \quad (20)$$

Here R_{tot} is the mass loss due to run-off and C_{tot} the mass loss due to calving, for the entire glacier (or drainage basin).

ACKNOWLEDGEMENTS

I thank T. Laumann, M. Kenneth and B. Wold for stimulating discussions on the mass balance of glaciers in Norway. Suggestions made by D. MacAyeal helped to improve the style of this paper. This work has been supported by the Commission of the European Communities (contract EPOC 0015).

REFERENCES

- Ambach, W. 1963. Untersuchungen zum Energieumsatz in der Ablationszone des grönländischen Inlandeises. *Medd. Grönl.*, **174**(4).
- Greuell, W. and J. Oerlemans. 1986. Sensitivity studies with a mass balance model including temperature profile calculations inside the glacier. *Z. Gletscherkd. Glazialgeol.*, **22**(2), 101–124.
- Haakensen, N., ed. 1982. Glasiologiske undersøkelser i Norge 1980. *Norges Vassdrags- og Elektrisitetsvesen. Vassdragsdirektoratet. Hydrologisk Avdeling. Rapport 1-82*.
- Kimball, B. A., S. B. Idso and J. K. Aase. 1982. A model of thermal radiation from partly cloudy and overcast skies. *Water Resour. Res.*, **18**, 931–936.
- Kraus, E. B. 1972. *Atmosphere-ocean interaction*. Oxford, Clarendon Press.
- Kuhn, M. 1979. On the computation of heat transfer coefficients from energy-balance gradients on a glacier. *J. Glaciol.*, **22**(87), 263–272.
- Müller, H. 1984. *Zum Strahlungshaushalt im Alpenraum*. Zürich, Technische Hochschule.
- Müller, M. J. 1987. *Handbuch ausgewählter Klimastationen der Erde*. Trier, Universität Trier.
- Oerlemans, J. 1986. An attempt to simulate historic front variations of Nigardsbreen, Norway. *Theor. Appl. Climatol.*, **37**, 126–135.

- Oerlemans, J. 1988. Simulation of historic glacier variations with a simple climate-glacier model. *J. Glaciol.*, **34**(118), 333–341.
- Oerlemans, J. 1991. The mass balance of the Greenland ice sheet: sensitivity to climate change as revealed by energy-balance modelling. *Holocene*, **1**(1), 40–49.
- Oerlemans, J. In press. A model for the surface balance of ice masses. Part I. Alpine glaciers. *Z. Gletscherkd. Glazialgeol.*
- Oerlemans, J. and N.C. Hoogendoorn. 1989. Mass-balance gradients and climatic change. *J. Glaciol.*, **35**(121), 399–405.
- Østrem, G., O. Liestøl and B. Wold. 1976. Glaciological investigations at Nigardsbreen, Norway. *Nor. Geogr. Tidsskr.*, **30**(4), 187–209.
- Østrem, G., K. D. Selvig and K. Tandberg. 1988. Atlas over breer i Sør-Norge. *Norges Vassdrags- og Energiverk. Hydrologisk Avdeling. Meddelelse* 61.
- Sauberer, F. 1955. Zur Abschätzung der Globalstrahlung in verschiedenen Höhenstufen der Ostalpen. *Wetter und Leben*, **7**, 22–29.

The accuracy of references in the text and in this list is the responsibility of the author, to whom queries should be addressed.

MS received 5 August 1991 and in revised form 11 November 1991